

An introduction to envelope constrained filter design

Antonio Cantoni, Ba-Ngu Vo, and Kok Lay Teo

Abstract — Envelope constrained filter design is concerned with the time domain synthesis of a filter whose response to a specified input signal stays within prescribed upper and lower bounds and in addition has minimal noise enhancement. In many practical applications, a “soft” approach, such as least mean square, is not the most suitable and it becomes necessary to use “hard” constraints such as the ones considered in the paper. We present an overview of key ideas related to robust continuous time envelope constrained filter design.

Keywords — filter, optimisation, constraints, envelopes, time domain, noise, robustness.

1. Introduction

In the continuous time envelope constrained (EC) filter design problem, we consider the design of a filter such that the noiseless response to a specified excitation fits into a prescribed envelope. Furthermore, we seek those filters that minimize a cost functional that is appropriate for the application of the filter.

Often in a time domain filter synthesis problem, the performance criterion used is the mean square error between the filter output and some desired signal. However, in many practical applications, this “soft” approach is not the most suitable and it becomes necessary to use “hard” constraints such as envelope constraints. Moreover, problems often arise in practice where it is crucial that the shaped signal fits into a prescribed envelope. The specifications of the output constraint envelope can arise either from standards set by certain regulatory bodies or practical design considerations. In telecommunications systems, pulse shapes used in transmission systems are specified by recommendations issued by standards bodies [1–4]. In sonar, radar ranging systems and imaging systems, the constraints arise from consideration of resolution and are associated with pulse compression technique requirements [5–8].

Over the past twenty years, the work on envelope constrained filters has evolved to take into account many engineering issues. In our overview, we present the key ideas related to robust continuous time envelope constrained filter design. Numerical methods for obtaining the solution to the problems formulated are not considered in this paper. The reader is referred to the following references for a range of efficient techniques for computing the optimal solution [9–18].

2. The envelope constrained filter applications

In this section, we briefly review a few applications that have motivated the study of envelope constrained filter design. The applications covered are by no means exhaustive and are intended to bring out a number of different aspects of the envelope constrained filter design problem.

2.1. Radar application

In radar and sonar, narrow pulses are required for range resolution and clutter reduction, but it is also important that the transmitted pulses contain sufficient energy for long-range detection. These two conflicting requirements would seem to dictate narrow pulses with high peak power. However, because of transmitter design considerations, peak power is limited, pulses of relatively long duration are transmitted and an operation known as **pulse compression** is performed at the receiver as illustrated in Fig. 1. This compression is most commonly achieved with a **matched filter**, that is, by correlating the incoming signal with the time-shifted and/or frequency shifted copies of the transmitted waveform. Matched filtering is well known to be optimal with respect to various performance criteria.

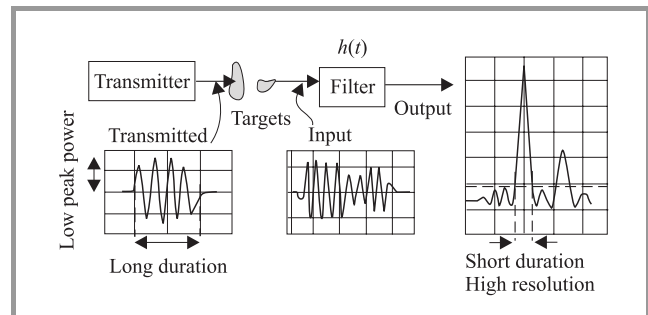


Fig. 1. Pulse compression.

The presence of a signal is detected when the matched filter output exceeds a threshold value, and parameters such as time delay and (Doppler) frequency shift are **estimated** by locating the peak output in time and frequency. If a signal s , non-zero on the interval $(t_0, t_0 + T)$, appears at the input to a pulse-compression filter, the output typically consists of a main peak surrounded by sidelobes, as shown in Fig. 1. When a radar must distinguish among multiple targets, these sidelobes can cause false detections and impede resolution of adjacent pulses. For example, if the transmitted pulse is a 13-bit Barker code and a matched filter

receiver is used, the output is compressed to 1/13 of the original pulse length, improving range resolution with no detection loss. Unfortunately, the output pulse is accompanied by 12 sidelobes, where the amplitude of each of these sidelobes is 1/13 of that of the main lobe peak. Thus, it is necessary in certain cases to remove or at least restrict the height of these sidelobes to an acceptable level. Of course there will be some noise penalty that results.

Problems of this type are often treated by using a least square approach, where the mean squared difference between the output and some desired pulse shape is minimized. If the sidelobes are reduced using a least square cost, there is no guarantee that the appearance of low-energy high-peak sidelobes (which can cause false detections) can be avoided. Moreover, the solution can be sensitive to the detailed structure of the desired pulse, and it is usually not obvious how the shape of the desired pulse should be altered in order to achieve better performance in terms of low level sidelobes.

The reduction of sidelobes can be formulated in terms of an envelope constrained problem: find the filter (if it exists) that causes least detection loss while reducing the output sidelobes to a specified fraction of the mainlobe peak. The envelope or pulse shape mask takes on the form shown in Fig. 2. Since the probability of detection is proportional to the signal to noise ratio, which in turn, is inversely proportional to the square of the norm of the filter, we are faced with the task of finding a minimum norm filter subject to the constraint that the sidelobe peaks remain within the specified values.

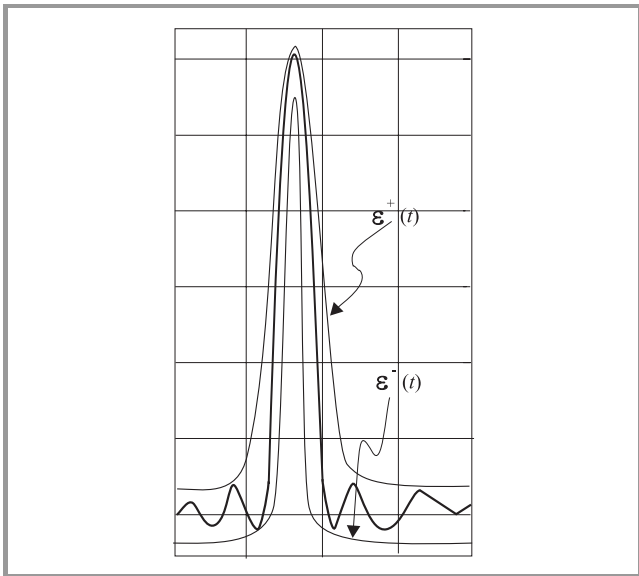


Fig. 2. Pulse shape constraints for radar/sonar problem.

2.2. Digital transmission application

In telecommunication standards, the performance of a digital link is often characterized by pulse masks applied to

the test pulses (see, for example, the CCITT recommendations [1, 2]). The signal s would correspond to the test signal specified in the standards. As an example, consider the equalization of an RG59B/U coaxial cable channel whose attenuation follows an approximate \sqrt{f} law (one with a 150 m length has approximately 12 dB loss at 70 MHz). The frequency response of a coaxial cable of length l is given by

$$H(j\omega) = e^{-Al\sqrt{j\omega}} = e^{-Al(\sqrt{\omega/2} + j\sqrt{\omega/2})}$$

Let A_0 denote the attenuation of the cable in dB at a frequency f_0 Hz. Then,

$$A_0 = (20Al \log e) \sqrt{\frac{\omega_0}{2}} = (20Al \log e) \sqrt{\pi f_0},$$

where $\omega_0 = 2\pi f_0$. The impulse response of the cable is given by

$$h(t) = \frac{Al}{2\sqrt{\pi t^3}} \exp\left(-\frac{A^2 l^2}{4t}\right), \quad t > 0.$$

A plot showing the impulse response for several values of Al is given in Fig. 3. Since Al increases with increasing cable length, the peak of the pulse in transit decreases and its base width widens as the cable lengthens. In order to successfully detect these pulses, the width must be compressed by means of pulse shaping networks at the receiving end.

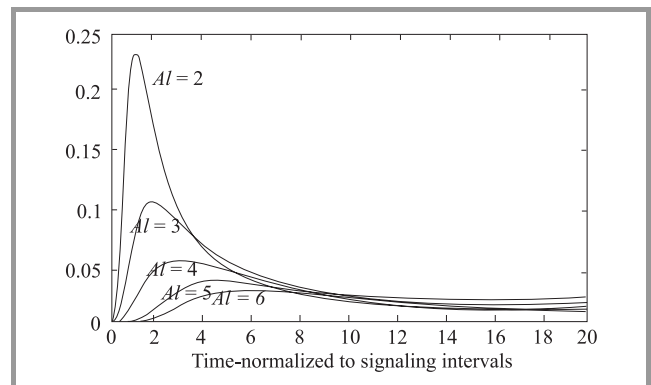


Fig. 3. Impulse response of coaxial cable for various lengths.

For a digital transmission channel consisting of a coaxial cable operating at the DX3 rate, i.e. 45 Mb/s (see [1, 2]), the American National Standards Institute (ANSI) specifies that at the pulse received, after transmission should fit in the mask illustrated in Fig. 4. From the characteristics of the cable shown in Fig. 3 it can be seen that for long cables the received pulse will not fit in the mask. An equalizing filter is required to shape the impulse response of the cable so that it fits in the envelope given by the DSX3 pulse template in Fig. 4. In Fig. 4 we have also shown the received pulse and the pulse at the output of an optimal EC filter. The cable has a 30 dB attenuation at frequency $2\pi/\beta$, where β denotes the baud interval ($22.35 \cdot 10^{-9}$ s).

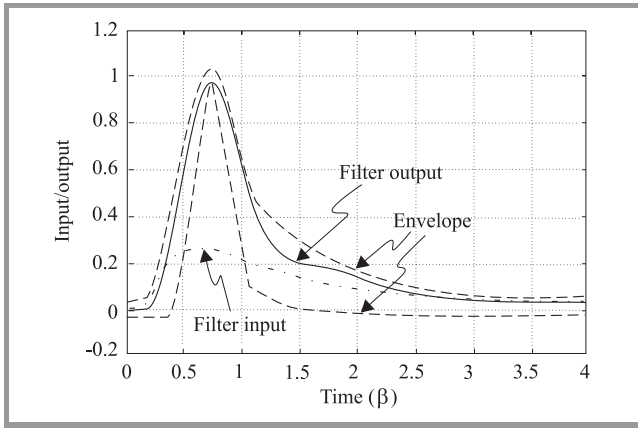


Fig. 4. DSX3 pulse template, coaxial cable and filter output.

Consider another transmission system example shown in Fig. 5, where a pulse pre-shaping filter is placed before the channel. When a rectangular pulse is transmitted, the noiseless output of the channel is required to fit into a T1 mask specified by the ANSI. The T1 baud rate is 1.544 Mb/s. It makes sense to minimize the norm of the pulse shaping filter to reduce the crosstalk to other signal as this is proportional to the transmit signal power.

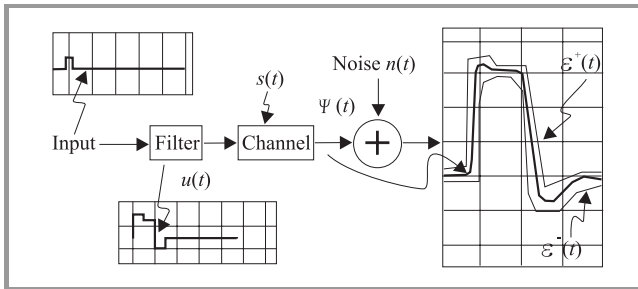


Fig. 5. Pre-shaping of pulse.

3. Formulation of optimal envelope constrained filters

In this section, we first introduce the basic EC filter design problem. This includes consideration of possible cost functionals for selecting the optimum filter. Then we expand the basic formulation by considering the problem of designing EC filters that are robust to signal modeling errors and filter implementation errors.

3.1. Basic envelope constrained filter design problem

We now formalize somewhat the definition of the EC filtering problem in its simplest form. The previous section has outlined some applications that motivated the study of the EC filtering problem without an explicit problem statement. This section presents a more precise statement that covers

all the applications previously discussed for both analog and hybrid filters.

3.1.1. Analog filters

Consider the filtering function shown in Fig. 6 be it for pulse compression or equalization. The excitation s entering the filter is corrupted by additive zero-mean, stationary noise n . The impulse response u of the linear time-invariant

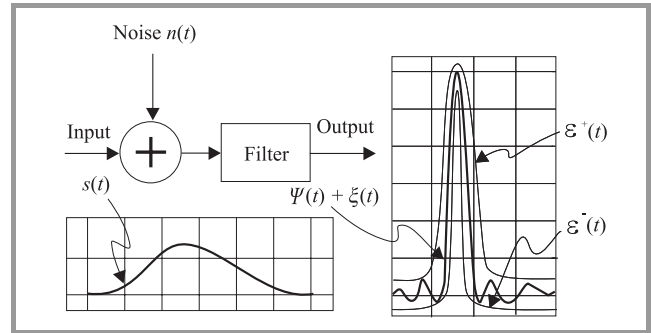


Fig. 6. Receiver model and output mask.

filter is to be determined and is restricted to be Lebesgue square-integrable on $[0, \infty)$. The output consists of two components ψ and ξ due to the signal and noise respectively. The noiseless output ψ is given by the convolution $s * u$:

$$\psi(t) = (s * u)(t) = \int_0^\infty s(t - \lambda) u(\lambda) d\lambda .$$

The notation Ξ_s is adopted to denote the mapping of u to the filter response $\psi = s * u$, i.e.

$$\Xi_s u = s * u . \tag{1}$$

Let ε^- and ε^+ be two piece-wise continuous functions of time representing the lower and upper boundaries of the output mask respectively. Then the envelope constraints require the filter output ψ to fit into a fully specified envelope as depicted in Fig. 6, i.e.

$$\varepsilon^-(t) \leq \psi(t) \leq \varepsilon^+(t), \quad \forall t \in \Omega \subset [0, \infty) . \tag{2}$$

Define

$$d = 0.5(\varepsilon^+ + \varepsilon^-) \text{ and } \varepsilon = 0.5(\varepsilon^+ - \varepsilon^-) .$$

Then (2) can be written as

$$|\Xi_s u - d| \leq \varepsilon .$$

So far we have defined the feasible region for the filters we wish to find. In many cases, the feasible region is not empty and there are many filters for which (2) holds. However, in many applications, there are other considerations that in fact lead us to select a specific filter. For example, it may be desirable to minimize the noise enhancement of the filter if the signal input to filter is corrupted by noise or it may

be necessary to minimize the filter output power to contain crosstalk. We consider in detail the noisy input case and define our cost function f to be the output noise power. Let ξ denote the noise component of the filter output. Then,

$$\xi(t) = \int_0^\infty n(t-\lambda)u(\lambda)d\lambda. \quad (3)$$

Assuming that the additive noise n at the receiver input is zero-mean, stationary, with autocorrelation $R_{nn}(\tau)$, the output noise power is:

$$f(u) = E[\xi^2(t)] = \int_0^\infty \int_0^\infty R_{nn}(\kappa-\lambda)u(\lambda)u(\kappa)d\kappa d\lambda. \quad (4)$$

By defining a linear operator L based on the autocorrelation function R_{nn} as

$$(Lu)(\lambda) = \int_0^\infty R_{nn}(\kappa-\lambda)u(\kappa)d\kappa \quad (5)$$

and using the usual inner product, the cost functional defined by Eqs. (1) and (4) can be expressed in a more convenient and intuitive form as a quadratic function of the filter impulse response:

$$f(u) = \langle u, Lu \rangle. \quad (6)$$

The cost functional is strictly convex when L is positive definite. In this case,

$$\|u\|_L \equiv \sqrt{\langle u, Lu \rangle}$$

is a norm.

Suppose that in addition to being additive, zero-mean and stationary, the input noise n is also **white**, with autocorrelation

$$R_{nn}(\tau) = N_0\delta(\tau),$$

where δ is a unit impulse. Then, the output noise power $E[\xi^2(t)]$, Eq. (4), is proportional to the square of the L_2 -norm of the filter,

$$\begin{aligned} E[\xi^2(t)] &= N_0 \int_0^\infty \int_0^\infty \delta(\kappa-\lambda)u(\lambda)u(\kappa)d\kappa d\lambda = \\ &= N_0 \int_0^\infty u^2(\lambda)d\lambda = N_0\|u\|_2^2. \end{aligned} \quad (7)$$

The cost functional in this case is strictly convex (not all norms are strictly convex), and L , defined by Eq. (5), is the identity operator.

In the derivation of the previous cost functionals, it is assumed that the statistics of the noise are known. In some applications, the exact noise statistics may not be known. We now consider one approach for dealing with this case.

Suppose that the noise spectral density is denoted as $\Phi_N(\omega)$. It can be verified that the output noise power due to the input noise n is given by

$$P_N = \frac{1}{2\pi} \int_{-\infty}^\infty \Phi_N(\omega)|U(j\omega)|^2 d\omega,$$

where U denotes the Laplace transform of u . Assume that Φ_N the noise power density satisfies

$$\|\Phi_N\| = \frac{1}{2\pi} \int_{-\infty}^\infty \Phi_N(\omega)d\omega \leq 1$$

but is otherwise unknown. It makes sense to consider the output noise power for the worst case input noise, i.e.

$$P_N = \max_{\|\Phi_N\| \leq 1} \frac{1}{2\pi} \int_{-\infty}^\infty \Phi_N(\omega)|U(j\omega)|^2 d\omega.$$

It can be shown [26], that

$$\|U\|_\infty^2 = \max_{\|\Phi_N\| \leq 1} \frac{1}{2\pi} \int_{-\infty}^\infty \Phi_N(\omega)|U(j\omega)|^2 d\omega, \quad (8)$$

where $\|U\|_\infty$ denotes the H_∞ -norm of U and is defined as $\|U\|_\infty = \sup_{\omega \in \mathbf{R}} |U(j\omega)|$.

Hence, minimizing the output noise power for the worst case input noise is equivalent to finding a filter of transfer function $U(s)$ with minimum H_∞ -norm. In this case, the cost functional can be expressed explicitly in terms of u as

$$f(u) = \left\| \int_0^\infty u(t)e^{-st} dt \right\|_\infty^2. \quad (9)$$

This cost functional is convex (but not strictly convex). In cases in which the input signal is subject to random disturbance with unknown but bounded power spectrum, the H_∞ optimization approach may offer a robust design.

The use of these and similar convex cost functionals can also be motivated by consideration of the filter's sensitivity to implementation errors and uncertainties in filter parameters.

3.1.2. Hybrid filters

Advances in the development of digital processors motivate the consideration of filter structures realized with digital components. A continuous-time filter can be implemented as a hybrid filter composed of an A/D converter, a discrete-time filter, a D/A converter and a post-filter. The EC design filter problem is to determine the discrete-time component of such a filter so as to minimize the effect of input noise whilst satisfying the constraint that the response of the filter to a specified signal fits into a prescribed mask.

The hybrid filter is shown in Fig. 7. The post-filter's function is to smooth the output of the D/A block. In other words, the combined function of the D/A block and the post-filter is to interpolate the (discrete-time) output of the digital processor. The absence of a post-filter corresponds to piece-wise constant interpolation of the digital output. Next on the ladder of complexity is linear interpolation. The output of the system varies from a staircase to much smoother waveforms depending on the type of interpolation. In practice, the post-filter is often implemented as a lowpass filter with cut-off frequency being half of the sampling frequency, for example, Butterworth, Bessel, Chebyshev and elliptic filters.

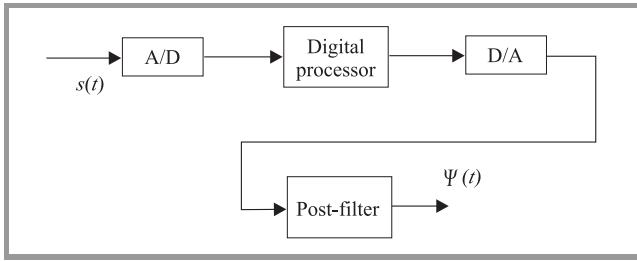


Fig. 7. Hybrid filter.

It is assumed that the incoming signal is sampled at or above the Nyquist rate. To simplify matters, quantization effects inherent in digital processes are neglected. This assumption results in a linear system.

Consider a digital processor that has a discrete-time impulse response $u \in l_2$. Then, the response of the hybrid filter to the continuous-time excitation x is given by

$$\psi(t) = \sum_{i=-\infty}^{\infty} \sum_{j=0}^{\infty} x[(i-j)\tau] u(j) \Lambda(t-i\tau), t \in [0, \infty), \quad (10)$$

where

$$\Lambda(t) = \int_0^{\infty} \Pi(\lambda) h(t-\lambda) d\lambda, \quad (11)$$

$$\Pi(t) = \begin{cases} 1, & t \in [0, \tau] \\ 0, & \text{otherwise} \end{cases} \quad (12)$$

and $h(t)$ is the impulse response of the post-filter.

Assuming appropriate post-filtering such that (10) converges for all $t \in [0, \infty)$ (e.g. bounded input bounded output stability). Then, ψ is bounded and continuous on $[0, \infty)$. Moreover, the mapping defined by

$$(\Xi_x u)(t) = \sum_{i=-\infty}^{\infty} \sum_{j=0}^{\infty} x[(i-j)\tau] u(j) \Lambda(t-i\tau) \quad (13)$$

is a continuous linear operator. The constraint set for this problem

$$\mathcal{F} = \{u \in l_2 : \varepsilon^- \leq \Xi_s u \leq \varepsilon^+\}$$

is thus convex. In analog or discrete filtering, the operator Ξ_x corresponds to a convolution by x under appropriate signal spaces.

A simple cost functional that one could use for the EC problem is the norm of the discrete-time filter. However, unlike the discrete-time the output noise power of the hybrid filter is not directly proportional to this norm. Assuming stationary input noise samples $n(i\tau)$, it can be shown that the output noise $\xi(t) \equiv (\Xi_n u)(t)$ is cyclo-stationary with period τ and that an appropriate well-defined cost for the EC problem with hybrid filter is the averaged output noise power given by

$$f(u) \equiv \frac{1}{\tau} \int_0^{\tau} E[\xi^2(t)] dt = \sum_{l=0}^{\infty} \sum_{m=0}^{\infty} u(l) u(m) L_{l,m}, \quad (14)$$

where

$$L_{l,m} = \frac{1}{\tau} \sum_{j=-\infty}^{\infty} \sum_{k=-\infty}^{\infty} R_{nn}((j-k)\tau) \times \int_0^{\tau} \Lambda[t-(j+l)\tau] \Lambda[t-(k+m)\tau] dt \quad (15)$$

and $R_{nn}((j-k)\tau)$ is the input noise autocorrelation.

3.2. Envelope constrained filtering problem

The EC filtering problem can be expressed as

$$\begin{aligned} & \min f(u) \\ & \text{subject to } |\Xi_s u - d| \leq \varepsilon, \end{aligned} \quad (16)$$

where ε^- and ε^+ are two continuous functions of time representing the lower and upper boundaries of the output mask respectively and an appropriate cost functional as discussed above is selected.

To eliminate output envelopes that permit the trivial solution $u = 0$, it is sufficient to assume the existence of an open subset I of Ω such that $\varepsilon^+(t)\varepsilon^-(t) > 0, \forall t \in I$. This means that there is an open interval where both the upper and lower boundaries have the same sign.

3.3. Robust envelope constrained filter design

Assuming that the set of feasible filters does not contain the origin, i.e. no trivial solution, and since we seek feasible filters with smallest possible norm, it follows that the optimum filter always lies on the boundary of the feasible set. This means the response of the optimum filter to the prescribed input touches the output envelope at some points. Consequently, it is to be expected that disturbances in the prescribed input or implementation error can cause the output constraints to be violated. The problem of designing filters that are robust to such disturbances or techniques for providing a guard band on the output mask are essential to the implementation of practical EC filters. Of course, the penalty for robustness is a possible increase in the cost functional.

Three robustness formulations are introduced in the following sections. The first incorporates input uncertainty into the constraints. We refer to this as the EC with uncertain input (ECUI). The second approach incorporates filter implementation uncertainty into the constraints. The third approach does not consider the source of the disturbances but deals with possible disturbances by forcing the filter output away from the envelope boundaries. We refer to this as the constraint robustness problem.

3.4. EC with uncertain input

The EC filtering problem with uncertain input (ECUI), [22], addresses the robustness to input disturbances by allowing for uncertainty in the input pulse (Fig. 8). Here the input s is not specified exactly, but is known to lie within an input envelope described by upper and lower boundaries

s^- and s^+ . The filter is required to fit the response of all excitations within the boundaries s^- and s^+ into the output mask. Of course, the penalty for robustness is the increased noise gain of the filter. For example in the radar sidelobe reduction problem, it is desirable to design a sidelobe reduction filter which is robust in the sense that its output sidelobes remains small even if the input signal is slightly different from the nominal input. In channel equalization, the ECUI approach can handle the case where the channel characteristics are not known exactly but are known within limits. Note that the EC filtering problem is a special case of the ECUI problem.

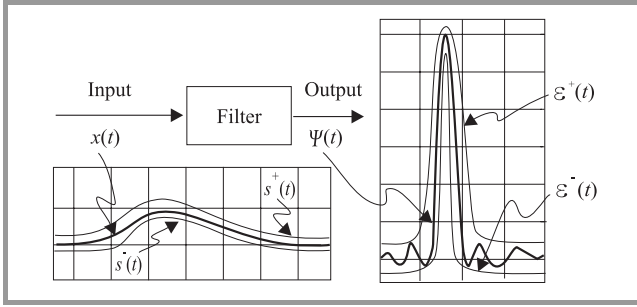


Fig. 8. EC filtering with uncertain input.

When the excitations are also constrained to stay within an envelope described by upper and lower boundaries s^+ , $s^- \in L_2[0, \infty)$. The feasible set F is given by

$$\mathcal{F} = \{u \in L_2[0, \infty) : |\Xi_x u - d| \leq \varepsilon, \forall x : |x - s| \leq \theta\}.$$

It can be shown that the feasible region \mathcal{F} is closed and convex. However, while the description of the feasible region in terms of the set of possible inputs is adequate for characterizing the problem it is not useful for computational purposes. To find out if a filter is feasible one would need to compute its response to every signal inside the input mask. There are no standard numerical techniques for handling problems with constraints of this form.

The following result has been established in [27].

Theorem 1: $|x * u - d| \leq \varepsilon, \forall x \in L_2[0, \infty) : |x - s| \leq \theta$ if and only if $|s * u - d| + \theta * |u| \leq \varepsilon$.

This result enables us to eliminate the perturbed input x from the original constraint expression and allows problem to be stated as follows:

$$\begin{aligned} & \min f(u) \\ & \text{subject to } G(u) = |\Xi_s u - d| + \Xi_\theta |u| - \varepsilon \leq 0. \end{aligned} \quad (17)$$

The cost functional and the constraint are continuous and convex function of the filter impulse response u . The parameters of this constraint function only involves the known signals d, ε, s and θ . Note that G is not always everywhere differentiable with respect to u .

3.5. Filter implementation uncertainty

In practice, it is often the case that a designed filter or system impulse response cannot be implemented exactly, there

are always implementation errors. These errors can arise from component mismatch or quantization of filter coefficients. So we are interested in finding filters which ensure that the envelope constraints are satisfied in the presence of implementation errors (if such filters exist).

It is assumed that for a given filter u , we can achieve actual implementations that are known to be within δ of u , where δ is a bounded function, i.e. any implementation of u belong to the set

$$\mathcal{V}(u, \delta) \equiv \{v \in L_2[0, \infty), |v - u| \leq \delta\}.$$

In the EC filtering problem we seek filters u whose responses to a prescribed signal s stay within some specified the output envelope. With uncertainty in the implementations, we are interested in those u such that the response of any elements of $\mathcal{V}(u, \delta)$ to the signal s stays inside the output envelope, i.e.

$$|\Xi_s v - d| \leq \varepsilon, \forall v : |v - u| \leq \delta. \quad (18)$$

Similar to the uncertain input problem, the description of the constraint is not very useful for computational purposes. We can show that the statement in (18) is equivalent to

$$|\Xi_s u - d| + |\Xi_s| \delta \leq \varepsilon. \quad (19)$$

Thus, to ensure robustness to implementation errors, we effectively tighten the output mask by reducing ε to $\varepsilon - |\Xi_s| \delta$.

Of course, if the uncertainty δ in the implementation is too large, the resulting output mask would not admit a feasible solution. We can determine from the implementation uncertainty δ whether robustness can be achieved. For instance, if there exists an interval $I \in [0, \infty)$ such that $(|\Xi_s| \delta)(t) \geq \varepsilon(t)$ for $t \in I$, then there is no feasible solution.

3.6. Constraint robustness

In this section, we present a technique for providing a guard band on the output mask and investigate how the trade-off between the noise gain and the constraint robustness can be achieved by proposing a new optimization problem. This is a generic approach which does not take into consideration the source or cause of the perturbation. Instead, we try to force the filter output to stay as far away from the mask as possible subject to some specified maximum allowable increase on the noise gain (Fig. 9).

For a given filter u (which may or may not satisfy the envelope constraints), consider the difference between its response $\Xi_s u$ and upper or lower mask boundary defined by

$$[\phi^+(u)](t) = (\Xi_s u)(t) - \varepsilon^+(t), \quad (20)$$

$$[\phi^-(u)](t) = \varepsilon^-(t) - (\Xi_s u)(t). \quad (21)$$

It is clear that if $\phi^+(u)$ and $\phi^-(u)$ are non-positive for all $\forall t \in \Omega$ then u satisfies the output constraints. To quantify

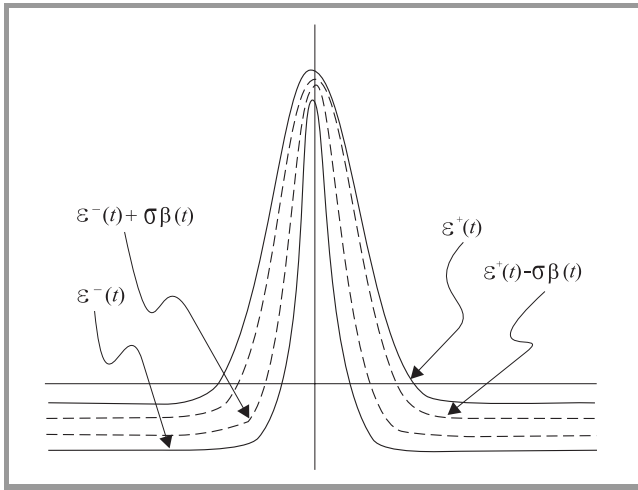


Fig. 9. Mask margins.

the notion of robustness we define its constraint robustness margin as

$$\rho(u) = \min \left\{ \min_{t \in \Omega} [-\phi^+(u)](t), \min_{t \in \Omega} [-\phi^-(u)](t) \right\}. \quad (22)$$

The feasible region of the EC filtering problem can now be expressed in terms of the robustness margin as

$$\mathcal{F} = \{u \in L_2[0, \infty) : \rho(u) \geq 0\}. \quad (23)$$

Moreover, if $\rho(u) > 0$, the minimum distance of the output $(\Xi_s u)(t)$ from the output mask is at least equal to $\rho(u)$. Therefore we may say that the filter u is robust with constraint robustness margin $\rho(u)$.

In practice, it may be necessary to have a larger constraint robustness margin over certain intervals. In this case, β can be used to specify the weightings in different time intervals. Define the weighted constraint robustness as follows:

$$\rho_\beta(u) = \min \left\{ \min_{t \in \Omega} \frac{[-\phi^+(u)](t)}{\beta(t)}, \min_{t \in \Omega} \frac{[-\phi^-(u)](t)}{\beta(t)} \right\}, \quad (24)$$

where β is a positive, piece-wise continuous function which is normalized so that it attains a minimum of unity on Ω_c and $\delta > 0$ is a constant which specifies the allowable amount of increase of the output noise power in the design of the optimal filter with maximum constraint robustness margin.

Let u^0 denote the optimal solution of the EC filtering problem without any additional robustness constraints, that is the solution to Eq. (16). The EC problem with robustness constraint is the following constrained optimization problem

$$\begin{aligned} & \max \rho_\beta(u) \\ & \text{subject to } \|u\|^2 \leq (1 + \delta) \|u^0\|^2. \end{aligned} \quad (25)$$

We can transform this to an equivalent problem as follows:

$$\begin{aligned} & \min f(u, \sigma) \equiv -\sigma \\ & \text{subject to } g_1(t, u, \sigma) \equiv \sigma\beta(t) - d(t) + \\ & \quad -\varepsilon(t) + (\Xi_s u)(t) \leq 0, \\ & g_2(t, u, \sigma) \equiv \sigma\beta(t) + d(t) - \varepsilon(t) - (\Xi_s u)(t) \leq 0, \\ & g_4(t, u, \sigma) \equiv \|u\|^2 - (1 + \delta) \|u^0\|^2 \leq 0. \end{aligned} \quad (26)$$

3.7. Theoretical foundation

From a mathematical point of view the following two theorems can be considered to capture all that one needs to know about the EC filtering problem defined in the previous sections.

Theorem 2: Let \mathcal{F} be a closed and convex subset in a Hilbert space H , and f a continuous and convex functional on H . If \mathcal{F} is non-empty, then there exists a $u^0 \in \mathcal{F}$ such that

$$f(u^0) \leq f(u), \quad \forall u \in \mathcal{F}.$$

Moreover, if f is strictly convex, then u^0 is unique.

Theorem 3: Let \mathcal{F} be a closed and convex subset of a separable Hilbert space H with non-empty interior \mathcal{F}^0 , and f a continuous and convex functional on H . Let u^0 be a minimum of f on \mathcal{F} and u_n^0 a minimum of f on $\mathcal{F} \cap [\{v_i\}_{i=0}^n]$, where $[\{v_i\}_{i=0}^\infty]$ denotes the linear span of $\{v_i\}_{i=0}^\infty$. If $\{v_i\}_{i=0}^\infty$ is total in H , then $f(u_n^0)$ monotonically decreases to $f(u^0)$ as n tends to infinity. Moreover, if f is an inner-product-induced norm, then

$$\lim_{n \rightarrow \infty} \|u_n^0 - u^0\| = 0.$$

Theorem 2 tells us about the existence of a solution and its uniqueness. Theorem 3 tells us about the convergence of finite structured filters to the optimal filter.

From a numerical analysts point of view, we would be concerned with the definition and characterization of algorithms for computing a solution. In fact, this aspect has been studied extensively both at a generic level and for the EC problem specifically, [10, 14–18, 20]. However, the treatment of these aspects is beyond the scope of this paper.

3.8. Finite filter structures

3.8.1. Analog filters

Suppose that one seeks to realize a filter by designing a network whose impulse response approximates that of the optimum EC filter in some sense, e.g. least squares, Páde, orthogonal approximations. The important question that arises is: would this approximation still satisfy the convex constraints? Thus, it would seem more appropriate to choose a particular filter structure and then impose the constraints. Sub-optimum solutions based on an appropriate choice of basis functions for the filter are likely to be more useful from a practical viewpoint.

Let $\{v_i\}_{i=0}^{\infty}$ be a total sequence in l_2 , and let the finite-structured filters have impulse responses given by $Ka \in l_2$, where $K: \mathbf{R}^n \rightarrow l_2$ is a bounded linear operator defined by

$$Ka = \sum_{i=0}^{n-1} a_i v_i = \mathbf{v}^T \mathbf{a},$$

where $\mathbf{v} = [v_0, v_1, \dots, v_{n-1}]^T$.

The feasible region, $F \cap [\{v_i\}_{i=0}^{n-1}]$, is hence embedded in an n -dimensional sub-space and can be characterized by the set of feasible filter coefficients which is defined in \mathbf{R}^n as

$$\{\mathbf{a} \in \mathbf{R}^n : \forall x \in S, x * (Ka) \in \Psi\}.$$

To obtain an explicit expression for the cost functional in terms of the vector of filter parameters \mathbf{a} , we have

$$f(K(\mathbf{a})) = \langle Ka, LKa \rangle = \mathbf{a}^T K^\dagger LK \mathbf{a},$$

where $K^\dagger: l_2 \rightarrow \mathbf{R}^n$ is the adjoint (operator) of K defined by $K^\dagger u = [v_0, u], \langle v_1, u \rangle, \dots, \langle v_{n-1}, u \rangle]^T$. The operator $K^\dagger LK: \mathbf{R}^n \rightarrow \mathbf{R}^n$ can be represented by the following $n \times n$ matrix, (often called a Gram matrix):

$$K^\dagger LK = \begin{bmatrix} \langle v_0, Lv_0 \rangle & \langle v_0, Lv_1 \rangle & \dots & \langle v_0, Lv_{n-1} \rangle \\ \langle v_1, Lv_0 \rangle & \langle v_1, Lv_1 \rangle & \dots & \langle v_1, Lv_{n-1} \rangle \\ \vdots & & \ddots & \vdots \\ \langle v_{n-1}, Lv_0 \rangle & \langle v_{n-1}, Lv_1 \rangle & \dots & \langle v_{n-1}, Lv_{n-1} \rangle \end{bmatrix}. \quad (27)$$

The Gram matrix $K^\dagger LK$ is positive semi-definite since L is positive semi-definite. Furthermore if L is positive definite and the v_i 's are linearly independent then $K^\dagger LK$ is also positive definite. In most practical situations, L is the identity operator and K is specified by a finite subset of a complete set of orthonormal v_i 's over the interval Ω_u . In this case it is easily seen that the Gram matrix $K^\dagger K$ is the identity matrix I . The main reason for considering filter realization by orthonormal sets is that it is possible to generate and combine certain set of vectors using simple finite filter structures. The most notable examples are Laguerre and Legendre functions.

There are two main techniques for building filters. The parallel structure is the simplest and most direct method (Fig. 10). The transfer function for each block is denoted by $\Theta_i(s), i = 0, 1, \dots, n-1$ and the transfer function of the filter is immediately given by

$$U(s) = \sum_{i=0}^{n-1} a_i \Theta_i(s).$$

In this case, $v_i = \theta_i$, where θ_i is the inverse Laplace transform of Θ_i . The parallel structure is widely used for many filters employing orthonormal functions.

The second method is the transversal structure (Fig. 11). The transfer function for each block is denoted by

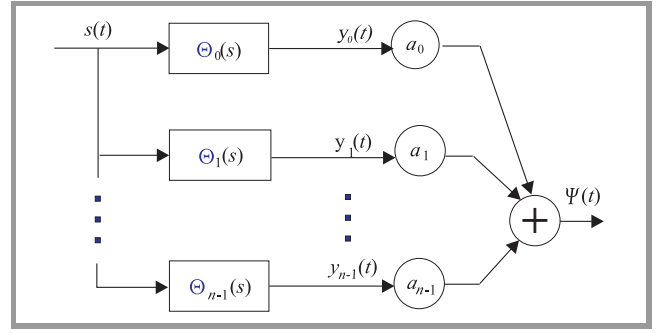


Fig. 10. Parallel filter structure.

$\Theta_i(s), i = 0, 1, \dots, n-1$. Let V_i denote the Laplace transform of v_i . Then

$$V_i(s) = \prod_{j=0}^i \Theta_j(s)$$

and the transfer function of the transversal filter is given by

$$U(s) = \sum_{i=0}^{n-1} a_i \prod_{j=0}^i \Theta_j(s).$$

The best known examples of filters employing the transversal structure are Legendre or Laguerre filters or when the Θ_i 's are pure delay elements.

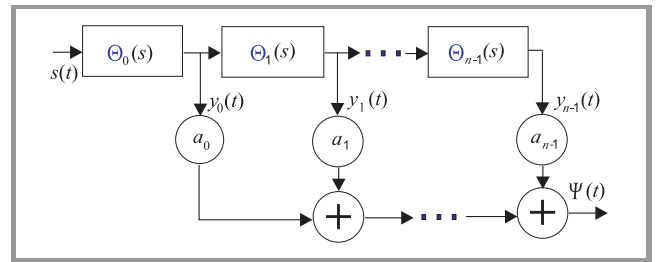


Fig. 11. Transversal filter structure.

These finite-structured filters restrict the space of filter impulse responses to a finite dimensional subspace of l_2 . That is, the optimization is carried out on this subspace rather than on the whole of l_2 . The subspace spanned by $\{v_i\}_{i=0}^{n-1}$ (denoted as $[\{v_i\}_{i=0}^{n-1}]$) is closed and convex, hence, the feasible region $\mathcal{F} \cap [\{v_i\}_{i=0}^{n-1}]$ is also closed and convex. Strict convexity of the cost functional ensures a unique optimum solution if an interior point exists. For a norm cost, it follows from Theorem 3: that the sub-optimum CCR filters for the finite filter structures converge to the optimum CCR filter as the filter structure grows. For a general convex cost, the sub-optimum costs converge to the optimum cost.

3.8.2. Hybrid filters

So far we have considered filters with impulse responses in l_2 . Now we narrow down the discrete-time filters to practical filters that have a finite structure.

Let $\{v_i\}_{i=0}^{\infty}$ be a total sequence in l_2 , and let the impulse response of finite filter structures be described by

$$u = Ka = \sum_{k=0}^{n-1} a_k v_k,$$

where $K : \mathbf{R}^n \rightarrow l_2$ is a bounded linear operator.

Such filters can be realized by FIR filter or discrete-time Laguerre networks where, incidentally, the corresponding v_k 's are also orthonormal. The set of feasible filter coefficients is given by

$$\{\mathbf{a} \in \mathbf{R}^n : \varepsilon^- \leq \Xi_s Ka \leq \varepsilon^+\}. \quad (28)$$

Assuming that the noise samples are statistically independent, the average output noise power can be expressed in terms of \mathbf{a} yielding the cost functional

$$f(Ka) = \mathbf{a}^T L \mathbf{a}, \quad (29)$$

where

$$L = (N_0/\tau) \int_{-\infty}^{\infty} \mathbf{w}(\zeta) \mathbf{w}^T(\zeta) d\zeta, \quad (30)$$

$$\mathbf{w}(t) = [w_0(t), \dots, w_{n-1}(t)]^T, \quad w_k(t) = \sum_{j=0}^{\infty} \Lambda(t - j\tau) v_k(j). \quad (31)$$

If the noise samples are independent, the cost functional $\mathbf{a}^T L \mathbf{a}$ is a strictly convex function of \mathbf{a} .

4. Numerical examples

In this section, we present three applications of EC filter design to illustrate the effectiveness of the techniques presented in the previous sections. The reader is referred to [9, 15] for many more examples.

4.1. EC with uncertain input

Consider the compression of a 13-bit Barker coded signal shown in Fig. 12.

For this example, we use a 27-tap FIR filter and a Bessel post-filter of 3th order with cut-off frequency $\omega_c = 2\pi/\beta$. To obtain the approximate solution, we have constrained the output at every $t_i = i\beta/8$. Figures 13 and 14 show, respectively, the filter's responses to the nominal input and signals which were randomly perturbed about the nominal input but still fit inside the input mask. Observe that these responses stay within the boundary of the output envelope. The noise gain of the ECUI filter is 0.027.

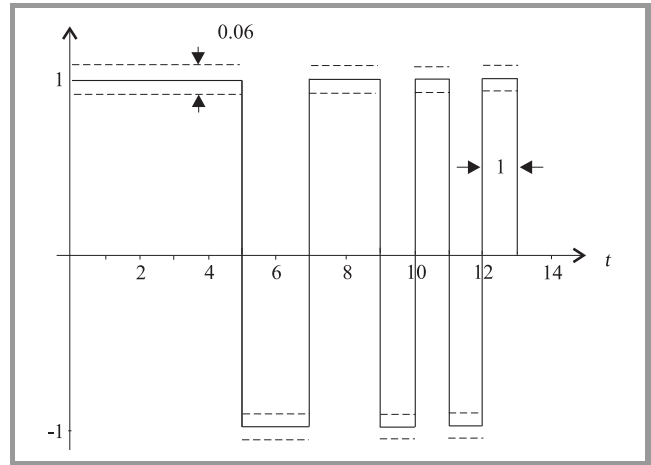


Fig. 12. 13-bit Barker code with input uncertainty.

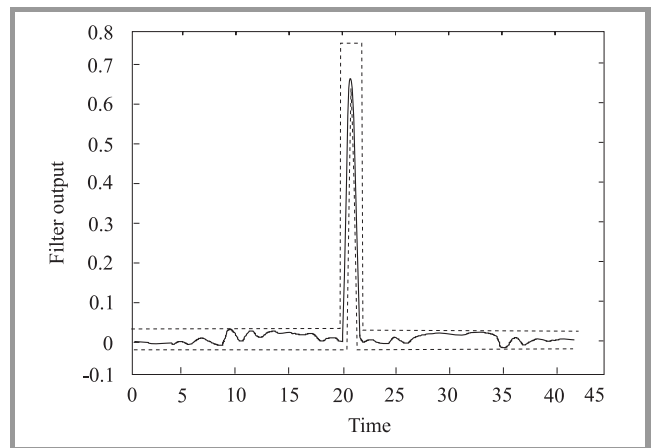


Fig. 13. Response of filter to nominal Barker coded input.

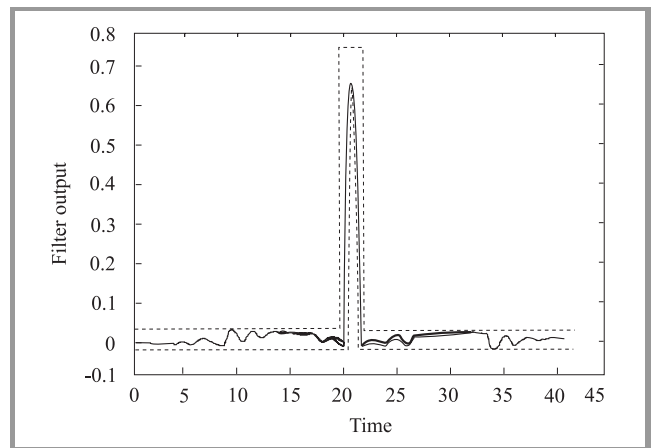


Fig. 14. Response of filter to perturbed Barker code.

4.2. Filter implementation uncertainty

The FALC54 is a Siemens IC for communications used in framing and line interface for PCM30 and PCM24. It

provides a very flexible way to create a custom waveform. Each pulse is partitioned into four subpulses of equal support as shown in Fig. 15. Hence, a pulse u generated from a FALC54 can be modeled as

$$u(t) = \sum_{k=0}^{n-1} x_k \Pi(t - kT/n),$$

where $n = 4$, Π denotes a rectangular pulse with support $[0, T/n]$ and x_k denotes the level of the k th subpulse. The shape of the transmit pulse is thus characterized by the vector of parameters $\mathbf{x} = [x_0, x_1, \dots, x_{n-1}]^T$. We are concerned with the problem of determining the levels of the transmit pulse to satisfy constraints which have arisen from the need to conform to standards such as ANSI, CCITT [3, 22].

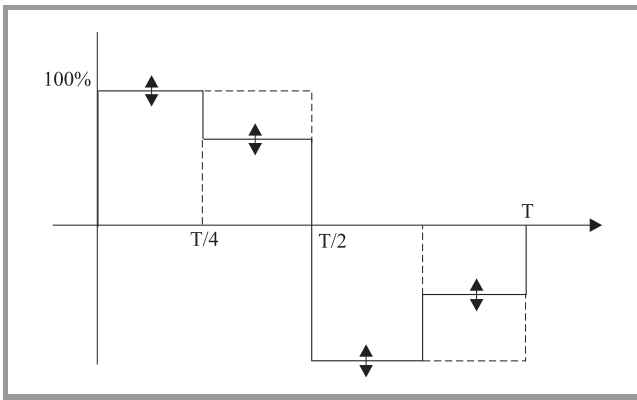


Fig. 15. Partition of pulse support.

Consider the transmission of the T1 pulse over an RG59B/U coaxial cable channel with an attenuation that follows an approximate \sqrt{f} law. For a coaxial cable of length l , its frequency response can be modeled as $H(j\omega) = e^{-Al\sqrt{j\omega}}$. Our design is for a length of a coaxial cable which has an attenuation of 4.5 dB at the DS1 rate $f_0 = 772$ kHz, (i.e. $\omega_0 = 4.8506 \cdot 10^6$ rad/s) and $T = 648 \cdot 10^{-9}$ s. We consider implementation errors on the transmit pulse shape that are bounded by $\mathbf{w} = 0.052[1, \dots, 1]^T$, i.e. $\delta = 0.052$.

Figure 16 shows the received signal at the end of the cable for an optimal transmit pulse design that does not take into account implementation errors bounded by $\delta = 0.052$. Note that for some implementation errors the received pulses violate the prescribed mask.

Figure 17 shows the received signal at the end of the cable for an optimal transmit pulse design that takes into account implementation errors bounded by $\delta = 0.052$ and uses the optimization problem formulated in Section 4.2. Note that the received pulses never violate the prescribed mask for any implementation error that satisfy the assumed bound. The robustness against implementation errors has been obtained at a very low cost of a 9% increase in the transmit pulse energy.

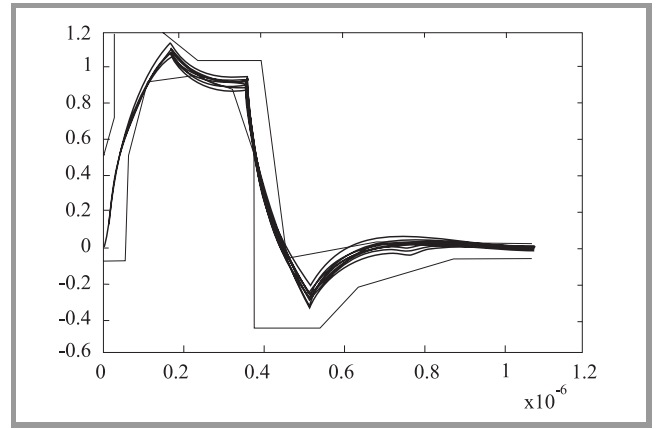


Fig. 16. Received pulse without implementation uncertainty constraints.

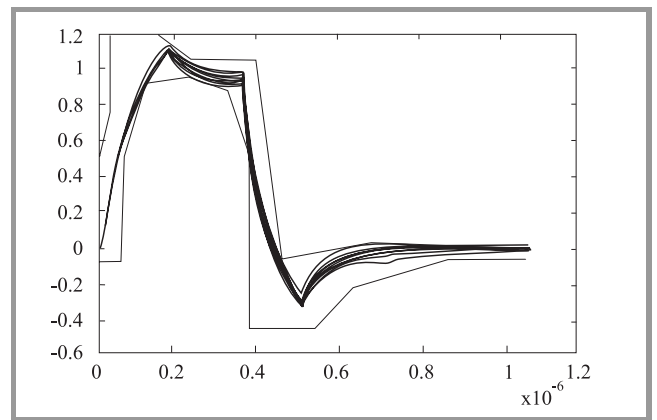


Fig. 17. Received pulse with implementation uncertainty constraints.

4.3. Constraint robustness with Laguerre filter

Let us again consider the design of an equalization filter for a digital transmission channel consisting of a coaxial cable on which data is transmitted according to the DX3 standard [2]. The design objective is to find an equalizer which takes the impulse response of a coaxial cable with a loss of 30 dB at the Baud frequency and produces an output which lies within the DSX3 pulse template. For computational purpose, we consider the time domain constraints at a finite number of discrete points rather than the entire continuum.

In our numerical studies, we use 1024 points over an interval of $[0, 32\beta]$. Using the Laguerre filter with 14 coefficients and $p = 12$, we first solve the optimal EC filtering problem without robustness considerations. The optimal noise gain is

$$\|u^0\|^2 = \|a^0\|^2 = 54.2008.$$

The output mask, input signal and the output are shown in Fig. 18.

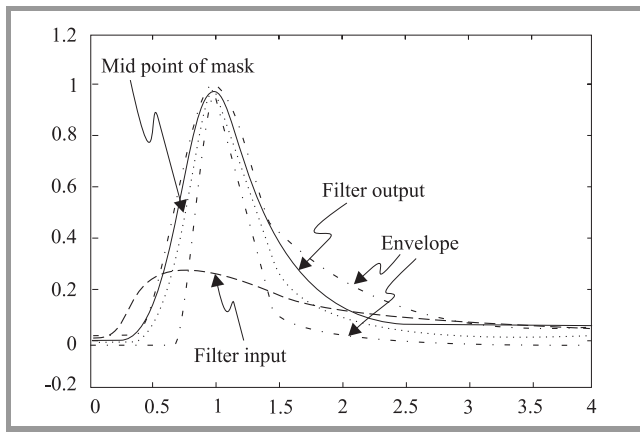


Fig. 18. Laguerre filter – EC approach.

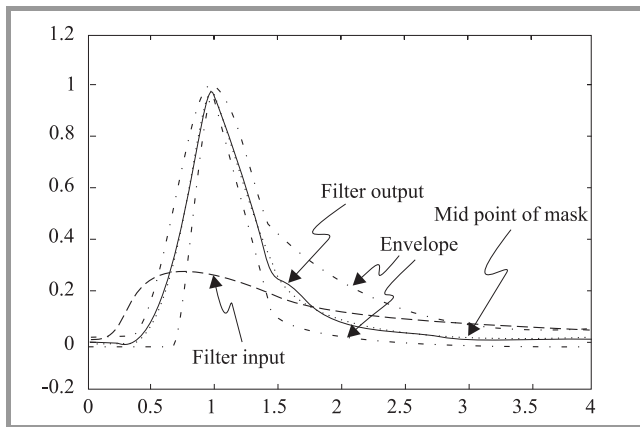


Fig. 19. Laguerre filter – EC approach with robustness constraints.

To achieve maximum constraint robustness margin, we solve the robust EC filtering problem with $\delta = 1.5$ and

$$\beta(t) = \begin{cases} 3\varepsilon(t), & |\varepsilon(t)| \geq 0.05 \\ 0.035, & |\varepsilon(t)| \leq 0.05 \\ \varepsilon(t), & \text{elsewhere} \end{cases}$$

The corresponding signals are shown in Fig. 19. From an examination of Fig. 19, we see that the output is very close to the center of the output mask. This increased margin has been achieved by allowing an increase of 50% in the noise gain of the robust EC filter relative to the noise gain of the non-robust EC filter ($\delta = 1.5$).

5. Conclusion

The paper has reviewed key ideas in envelope constrained filter design. We have shown that the design problem is motivated by practical engineering requirements. A number of filter design examples have been described. These examples include filters for communications systems and pulse compression applicable to sonar and radar ranging systems. The effectiveness of the robust EC filter design

approach presented in the paper is evident in these examples.

References

- [1] Bell Communications, Technical Reference, TR-TSY-000499, Dec. 1988, issue 2, pp. 9–17.
- [2] CCITT, “Physical/Electrical Characteristics of Hierarchical Digital Interfaces”, G.703, Fascicle III, 1984.
- [3] R. A. Nobakht and M. R. Civanlar, “Optimal pulse shape design for digital communication systems by projections onto convex sets”, *IEEE Trans. Commun.*, vol. 43, pp. 2874–2877, 1995.
- [4] J. W. Lechleider, “A new interpolation theorem with application to pulse transmission”, *IEEE Trans. Commun.*, vol. 39, no. 10, pp. 1438–1444, 1991.
- [5] R. J. McAulay and J. R. Johnson, “Optimal mismatched filter design for radar ranging detection and resolution”, *IEEE Trans. Inform. Theory*, vol. 17, pp. 696–701, 1971.
- [6] A. W. Rihaczek, *Principles of High-Resolution Radar*. New York: Macro-Hill, 1969.
- [7] A. Seyler and J. Potter, “Waveform testing of television transmission facilities”, in *Proc. IRE*, Australia, July 1960, pp. 470–478.
- [8] Z. L. Budrikis, “Visual fidelity criterion and modelling”, *Proc. IEEE*, vol. 60, no. 7, pp. 771–779, 1972.
- [9] B. Vo, “Optimum envelope constrained filters”, Ph.D. thesis, ATRI, Curtin University of Technology, Western Australia, Jan. 1997.
- [10] T. E. Fortmann and M. Athans, “Optimal filter design subject to output sidelobe constraints: theoretical considerations”, *JOTA*, vol. 14, no. 2, pp. 179–197, 1974.
- [11] D. G. Luenberger, *Optimization by Vector Space Methods*. New York: Wiley, 1969.
- [12] E. Polak and D. Q. Mayne, “An algorithm for optimization problems with functional inequality constraints”, *IEEE Trans. Automat. Contr.*, vol. 21, pp. 184–193, 1976.
- [13] G. Gonzaga, E. Polak, and R. Trahan, “An improved algorithm for optimization problems with functional inequality constraints”, *IEEE Trans. Automat. Contr.*, vol. 25, pp. 49–54, 1980.
- [14] B. Vo, A. Cantoni, and K. L. Teo, “Computational methods for a class of functional inequality constrained optimization problem”, in *World Scientific Series in Applicable Analysis – Recent Trends in Optimization Theory and Applications*, R. P. Agarwal, Ed. Singapore: World Scientific Publishing, 1995, vol. 5, pp. 447–465.
- [15] R. J. Evans, T. E. Fortmann, and A. Cantoni, “Envelope-constrained filter”. Part I. “Theory and applications”, *IEEE Trans. Inform. Theory*, vol. 23, pp. 421–434, 1977.
- [16] R. J. Evans, A. Cantoni, and T. E. Fortmann, “Envelope-constrained filter”. Part II. “Adaptive structures”, *IEEE Trans. Inform. Theory*, vol. 23, pp. 435–444, 1977.
- [17] W. X. Zheng, A. Cantoni, B. Vo, and K. L. Teo, “Recursive procedures for constrained optimization problems and its application in signal processing”, *IEE Proc. – Vision, Image Signal Proc.*, vol. 142, no. 3, pp. 161–168, 1995.
- [18] T. E. Fortmann and R. J. Evans, “Optimal filter design subject to output sidelobe constraints: computational algorithm and numerical results”, *JOTA*, vol. 14, no. 3, pp. 271–290, 1974.
- [19] L. R. Rabiner and B. Gold, *Theory and Application of Digital Signal Processing*. New Jersey: Prentice-Hall, 1975.
- [20] B. Vo, Z. Zang, A. Cantoni, and K. L. Teo, “Continuous-time envelope constrained filter design via orthonormal filters”, *IEE Proc. – Vision, Image Signal Proc.*, vol. 142, no. 6, pp. 389–394, 1995.
- [21] B. Vo, T. Ho, A. Cantoni, and V. Sreeram, “FIR filters in continuous-time envelope constrained filter design”, in *Proc. IEEE ICASSP*, Munich, Germany, 1997, vol. 3, pp. 1905–1908.

- [22] R. J. Evans, A. Cantoni, and K. M. Ahmed, "Envelope-constrained filters with uncertain input", *Circ. Syst. Signal Proc.*, vol. 2, no. 2, pp. 131–154, 1983.
- [23] K. L. Teo, A. Cantoni, and X. G. Lin, "A new approach to the optimization of envelope constrained filters with uncertain inputs", *IEEE Trans. Signal Proc.*, vol. 42, no. 2, pp. 426–428, 1994.
- [24] W. X. Zheng, A. Cantoni, and K. L. Teo, "Robust design of envelope constrained filters in the presence of input uncertainty", *IEEE Trans. Signal Proc.*, vol. 44, no. 8, pp. 1872–1878, 1996.
- [25] W. Zheng, A. Cantoni, and K. L. Teo, "The sensitivity of envelope-constrained filters with uncertain input", *IEEE Trans. Circ. Syst. – I*, vol. 42, no. 9, 1995.
- [26] B. A. Francis, "A course in H_∞ control theory", in *Lecture Notes in Control and Information Sciences*, M. Thomas and A. Wyner, Eds. Berlin: Springer Verlag, 1987.
- [27] B. Vo and A. Cantoni, "Continuous-time envelope constrained filter design with input uncertainty", *IEEE Trans. Circ. Syst. – I*, vol. 47, no. 10, pp. 1445–1454, 1995.

Antonio Cantoni (FIEEE, FTSE) was born in Soliera, Italy, on 30 October, 1946. He received the B.E. (first class honours) and Ph.D. degrees from the University of Western Australia, Nedlands, in 1968 and 1972, respectively. He was a Lecturer in Computer Science at the Australian National University, Canberra, in 1972. He joined the Department of Electrical and Electronic Engineering at the University of Newcastle, Shortland, NSW, Australia in 1973, where he held the Chair of Computer Engineering until 1986. In 1987, he joined QPSX Communications Ltd, Perth, Western Australia, as Director of the Digital and Computer Systems Design Section for the development of the DQDB Metropolitan Area Network. From 1987 to 1990 he was also a visiting Professor in the Department of Electrical and Electronic Engineering at the University of Western Australia. From 1992 to 1997 he was the Director of the Australian Telecommunications Research Institute and Professor of Telecommunications at Curtin University of Technology, Perth, Western Australia. During this period he was also the director of the Cooperative Research Centre for Broadband Telecommunications and Networking. He is currently Chief Technology Officer with Atmosphere Networks Inc and Professor of Telecommunications at the University of Western Australia. He is interested in adaptive signal processing, electronic system design, and networking and regularly acts as a consultant to industry in these areas. Dr Cantoni is a Fellow of the IEEE and

a Fellow of the Australian Academy of Technological Sciences and Engineering. He has been an associate editor of the IEEE Transactions on Signal Processing.
e-mail: cantoni@ec.uwa.edu.au
University of Western Australia
Australia

Ba-Ngu Vo (MIEEE) was born in Saigon Vietnam. He received the B.Sc./B.E. degree (with first class honours) in 1994 from the University of Western Australia and his Ph.D. degree in 1997 from the Australian Telecommunications Research Institute (ATRI), Curtin University of Technology. He is currently a research fellow at the Department of Electrical and Electronic Engineering, the University of Melbourne. His research interests lie in the application of optimization techniques to signal processing, semi-infinite programming, filter design, tracking and data fusion.
e-mail: bv@ce.mu.oz.au
The University of Melbourne
Australia

Kok Lay Teo received the Ph.D. degree in electrical engineering from the University of Ottawa, Ottawa, ON, Canada in 1974. He was with the Department of Applied Mathematics, the University of New South Wales, Sydney, Australia, from 1974 to 1985, as a Lecturer and subsequently as a Senior Lecturer. He was an Associate Professor in the Department of Industrial and Systems Engineering, National University of Singapore from 1985 to 1987. He was an Associate Professor in the Department of Mathematics, The University of Western Australia, Nedlands, Australia, from 1988 to 1996. He was Professor of Applied Mathematics at Curtin University of Technology, Perth, Australia, from 1996 to 1998. He is currently the Chair Professor of Applied Mathematics and Head of the Department of Applied Mathematics at The Hong Kong Polytechnic University, Hong Kong. He has delivered 6 keynote lectures, 4 fully funded invited lectures, and published 4 books and numerous journal and conference papers. The software package, MISER3.2, for solving general constrained optimal control problems was developed by the research team under his leadership. His research interests include both the theoretical and practical aspects of optimal control and optimization, and their applications, in particular, to signal processing in telecommunications.
e-mail: teo@maths.curtin.edu.au
The Hong Kong Polytechnic University
Hong Kong